23rd International Conference on Renewable Energies and Power Quality (ICREPQ'25)
Tenerife (Spain), 25th to 27th June 2025
Renewable Energy and Power Quality Journal (RE&PQJ)
ISSN 2172-038 X, Volume No.23, September 2025

Adaptive VSG-based grid forming controller for optimal damped response under dynamic grid conditions

A. Ordono[1], J. Rodriguez-Gongora[2], A. Rubio-Egaña[1], A. Sanchez-Ruiz[3], P. Fernández-Bustamante[4], F.J Asensio[1], O. Lopez-de-Suso[3], A. Gomez-Raya[3]

[1] Department of Electrical Engineering
Faculty of Engineering, Gipuzkoa, University of the Basque Country (UPV/EHU)
Avda. Otaola, 29, 20600 Eibar (Spain)
Phone/Fax number: +34 943 033036, e-mail: ander.ordono@ehu.eus

[2] Electronics and Computing Department
Mondragon Unibertsitatea
Loramendi 4, 20500, Mondragon (Spain)

[3] Department of Electronic Technology
Faculty of Engineering Vitoria-Gasteiz, University of the Basque Country (UPV/EHU)
Nieves Cano 12, 01006 Vitoria-Gasteiz (Spain)

[4] Department of Electrical Engineering
Faculty of Engineering Vitoria-Gasteiz, University of the Basque Country (UPV/EHU)
Nieves Cano 12, 01006 Vitoria-Gasteiz (Spain)

Abstract. Grid forming inverters are a promising technology to ensure the stability of weak grids. One typical strategy is the virtual synchronous generator (VSG) approach, which mimics the swing equation of synchronous generators. This strategy can provide inertia, primary frequency regulation and damping to the grid. However, in classical VSG structures, these three characteristics cannot be managed independently, and damping is usually limited. This work proposes a modified VSG controller, which adds a derivative term in the active power feedback, in order to provide an extra degree of freedom. This strategy enables the independent control of frequency services: damping, frequency regulation and inertia. Moreover, as the damping is affected by the impedance of the grid, an adaptive control strategy is proposed. By estimating the grid reactance and adapting the derivative term, the controller can ensure the desired damping along all operational conditions.

Key words. Adaptive controller, grid forming, virtual synchronous generator

1. Introduction

With the global push for renewable energy, the penetration of power converters into the grid has increased significantly over the past few years. In parallel, the total amount of synchronous generation has been gradually reduced due to the closure of fossil-fuel-based energy plants. As a result, the power grid is becoming weaker both in terms of voltage stiffness and inertial response [1].

Traditionally, the integration of power converters has been based on grid-following (GFL) philosophy. In GFL mode, converters behave as a controlled current source synchronized with the grid by means of a Phase-Locked-Loop (PLL). The PLL estimates the angle of the voltage vector at the point of connection, known as Point of Common Coupling (PCC). This control approach exhibits good performance in stiff power grids, where the voltage at the PCC is uniquely imposed by the grid and not perturbed by the current injection of the converter. However, in weak grids, current injection and voltage become coupled due to the bigger grid impedance. In these circumstances, GFL becomes unsuitable for converter integration because of the stability issues associated to poor PLL tracking performance [2].

Grid-forming (GFM) philosophy has been recently proposed as a promising solution to enhance converter stability in weak grids [3]. In this mode, the converter behaves as a voltage source that imposes the voltage and the frequency, without the need of a PLL for synchronization. In literature, different control strategies for GFM converters have been suggested [4], among which the Virtual Synchronous Generator (VSG) is one of the most widespread [5].

VSG aims at emulating the swing equation of a synchronous generator (SG). However, unlike traditional machines, the behaviour of the virtual machine is not limited by physical constraints, such as actuator delays. The main advantage of this flexibility is that they enable faster response times compared to conventional SGs [6]. Nevertheless, VSG also lacks some beneficial characteristics of SGs, like damping windings, which are crucial for machine stability [7]. As a result, the damping

of the system becomes dependent on the primary frequency regulation capability, the inertia constant and the grid impedance. Due to this coupling effect, the stability of the system is compromised at certain operating conditions, where transient oscillations may be undesirably poorly damped [8].

This works proposes a modified VSG, which includes an additional degree of freedom to effectively manage the damping of the system. This is achieved by adding a derivative term to the active power feedback of the classic structure. However, damping is still affected by changes in grid impedance, leading to undesired under or overdamping. Hence, estimating a proper value of the grid impedance can help the converter control to adapt and properly auto-tune. Grid impedance estimation can be carried out in many ways, although a clear trend in the references is based on the injection of a controlled perturbation and an observation or measuring method [9]. Thus, it is assumed that the converter is able to know the grid fundamental frequency impedance value, obtained with any of the existing methods in the literature. With this approach, the derivative term can be adjusted to ensure a proper damping regardless of the operational conditions of the system.

The structure of this paper is as follows. Section 2 provides a description of the topology of the system including the explanation of the classical VSG controller. In Section 3 the small-signal model of the system is derived and analysed. Section 4 presents the adaptive VSG controller and in Section 5 simulation results are included. Finally, conclusions are addressed in Section 6.

2. Virtual Synchronous Generator based GFM inverter

A. Topology

In the context of renewable energy systems, a grid-connected converter represents an essential component. The converter typically functions in a back-to-back configuration with a shared DC bus, thereby allowing flexibility in the handling of diverse energy types.

At the primary stage, the source-side converter may be a DC/DC for solar energy, regulating the voltage level to the common DC bus, or an AC/DC used in wind energy to convert the variable-frequency AC to DC. The second stage, or the inverter, uses the energy from the DC bus and converts it to AC, synchronizing its output with the grid voltage. The present article is concerned exclusively with the second stage control, where GFM philosophy will be implemented. Thus, an ideal and constant DC source is considered for the analysis.

The simplified one-line diagram of the proposed GFM inverter is shown in Figure 1. The connection of the converter to the PCC is made by means of LC filter, which is usually designed to fulfil grid connection power quality demands. The LC filter can also include a damping resistor R_f to prevent filter resonance issues. For the sake of simplicity, the grid is modelled as an equivalent Thevenin circuit, composed of a voltage source and a series RL branch.

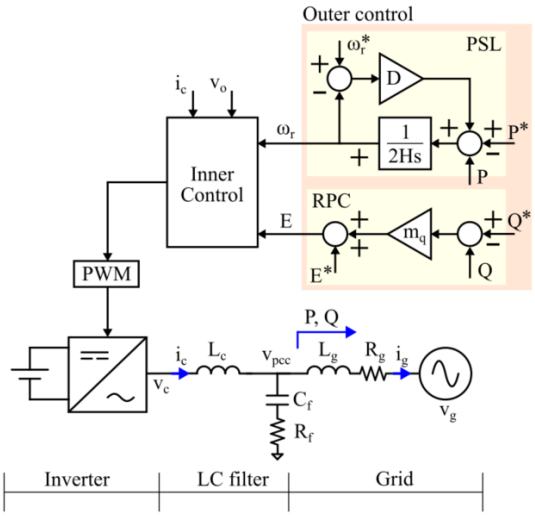

Figure 1 Schematic of a grid-connected GFM.

B. Controller

There exist a wide variety of different GFM control structures. However, all of them are typically composed of two layers: an inner and outer controller. The control structure is included in Figure 1.

The inner control layer is usually composed of a cascaded control structure, based on a dual loop voltage-current controller [10]. The voltage controller compensates the voltage drop in the filter impedance, providing GFM capability at the PCC. The converter current control can be used to protect the inverter under overloads. Since this article will focus on the VSG strategy and dynamics, a GFM without inner controllers will be considered.

The outer layer of GFM structures is related to the control of both the voltage amplitude and the output frequency of the GFM equivalent voltage source. In this sense, two separate control loops are typically distinguished: the Power Synchronization Loop (PSL) and the Reactive Power Control (RPC).

The PSL generates the output frequency ω_r based on measured active power P and active power and frequency references, P^* and ω_r^*. The diagram shows the classical VSG structure in per unit notation, which includes an inertia constant H (seconds), a damping term D. In the classical VSG structure, this damping term also determines the primary frequency regulation or power sharing capability of the inverter. In fact, this damping term is inversely related to the droop coefficient [4].

The RPC will generate the voltage amplitude E based on measured reactive power Q and reactive power and voltage amplitude references, Q^* and E^*. The diagram shows a reactive power droop approach. It is important to note that even if the RPC is a relevant element of GFM inverters, this paper will focus on the frequency dynamics.

Hence, the focus of this work are the PSL-associated dynamics.

3. Small-signal modelling and analysis

A simple approach to evaluate the active power dynamics of GFM inverters is to use a quasi-stationary model. In this approach, the grid is considered purely inductive, and impedance transient terms are neglected, so that the active power is determined by:

$$P = \frac{E|v_g|}{X_{eq}} \cdot \sin\delta \tag{1}$$

Where E and $|v_g|$ are the amplitudes of the GFM and the grid equivalent voltage sources, δ is the phase shift between both voltage sources, and X_{eq} is the overall reactance. Without inner controller, the overall reactance is the sum of the filter reactance and grid reactance $X_{eq} = X_c + X_g$. All the values in (1) are in per unit, except for δ, which is in radians.

By linearizing the previous equation and considering that the inverter and the grid operate close to their rated voltage values (1 pu), the relation between the active power and the phase shift is determined by the synchronization constant K_t, inversely related to the overall reactance:

$$\Delta P \cong \frac{1}{X_{eq}}\Delta\delta = K_t\Delta\delta \tag{2}$$

The quasi-stationary small-signal model for the grid-connected VSG is represented in Figure 2. The term ω_b is the base angular frequency (rad/s). This model is valid for evaluating the performance of PSLs in the low frequency range, between 0 and 20 Hz, as it neglects transient impedance terms [11].

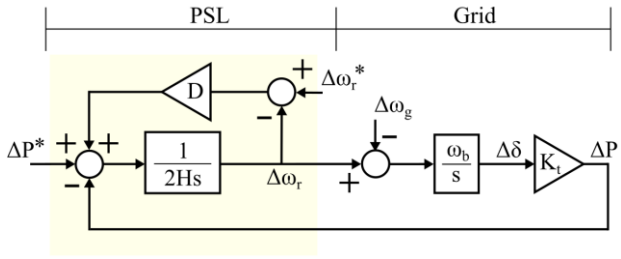

Figure 2. Quasi-stationary signal model of a grid-connected VSG

Neglecting the dynamics of the angular frequency setpoint ($\Delta\omega_r^* = 0$), two different transfer functions can be obtained for the grid-connected inverter. The first one determines the response to power setpoints ($\Delta P/\Delta P^*$), the second one is related to the response to grid frequency perturbations ($\Delta P/\Delta\omega_r$). These transfer functions are given by (3) and (4), respectively.

$$\frac{\Delta P}{\Delta P^*} = \frac{\omega_b K_t}{2Hs^2 + Ds + \omega_b K_t} \tag{3}$$

$$\frac{\Delta P}{\Delta w_g} = -\frac{\omega_b K_t(2Hs + D)}{2Hs^2 + Ds + \omega_b K_t} \tag{4}$$

The primary frequency regulation capability of the VSG can be determined from (4). It is determined by the active power variation under a steady-state grid frequency deviation. The active power variation under a unitary frequency step is obtained by applying the final value theorem in (5). In the classic VSG, the primary frequency regulation or power sharing capability of the inverter is exclusively determined by the damping D.

$$\Delta P = \lim_{s\to 0} s\left(\frac{\Delta P}{\Delta\omega_g}\right)\frac{1}{s} = -D \tag{5}$$

Both (3) and (4) transfer functions are also characterized by a second order system denominator. The natural frequency ω_n and damping δ of its poles depend on the inertia constant and damping term of the VSG, as well as on the synchronization constant (and hence, on grid impedance):

$$\omega_n = \sqrt{\frac{\omega_b K_t}{2H}} \tag{6}$$

$$\delta = \frac{D}{2\sqrt{2H\omega_b K_t}} \tag{7}$$

In VSG, H is usually determined to provide some inertial contribution to the grid. As the inertia is inversely related to the natural frequency (6), increasing the inertia makes the system slower or "heavier" for frequency fluctuations as in a conventional SG. On the other hand, D term is usually limited in order to ensure a proper power sharing among all the sources, according to (5). However, D also determines the damping of the system. Higher values of D will contribute to damping the system, but they will imply greater power contribution to frequency perturbations, which may lead to overload if the power rating of the converter is too small. Therefore, a trade-off between both is more than often necessary.

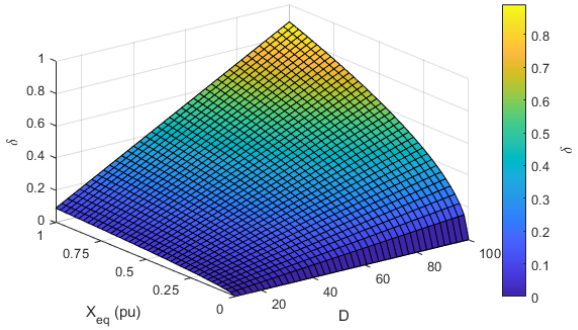

Figure 3. δ of grid-connected VSG under different D and K_t values. H = 5 s.

The main drawback of classic VSG structure is that it only provides two degrees of freedom, D and H, to preside over three parameters of the system: the inertia/natural frequency, the damping and the primary frequency regulation/power sharing capability. Hence, one of them will be dependent on the others. For instance, when the inertia constant of the VSG is fixed, the damping

coefficient will increase as D is increased. Additionally, the damping will be deteriorated as the grid impedance increase. Figure 3 provides a visual insight into the effect of D and X_{eq} variations on the damping coefficient of a VSG with an inertia constant of 5 s.

4. Modified VSG with adaptive capability

To prevent the coupling effect that arises in classical VSG PSL structure, an additional control parameter is needed to independently tune the damping of the system regardless of the inertia and/or primary frequency regulation. This work proposes the addition of a derivative term in the active power feedback of classic VSG. The proposed approach is shown Figure 4. This derivative term has a gain k_d, filtered through a low pass filter τ_d to limit the noise amplification related to the derivative.

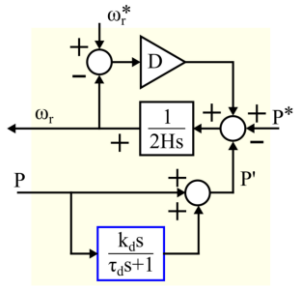

Figure 4. Modified VSG structure

The small-signal model of the modified VSG is shown in Figure 5. The constant time τ_d is usually tuned to filter high frequency components well-above 20 Hz, and hence, it can be neglected for the quasi-stationary model. Hence, the power feedback, which had an original gain of 1 in the conventional VSG, turns into $k_d s + 1$ in the modified VSG.

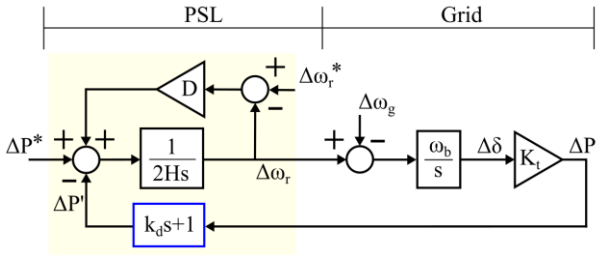

Figure 5. Quasi-stationary signal model of the modified VSG structure

The transfer functions that determine active power dynamics under setpoints and grid frequency perturbations are now:

$$\frac{\Delta P}{\Delta P^*} = \frac{\omega_b K_t}{2Hs^2 + (D + k_d \omega_b K_t)s + \omega_b K_t} \tag{8}$$

$$\frac{\Delta P}{\Delta \omega_g} = -\frac{\omega_b K_t (2Hs + D)}{2Hs^2 + (D + k_d \omega_b K_t)s + \omega_b K_t} \tag{9}$$

From the previous equations, it is observed that the derivative term only modifies the s term of denominator. Hence, it will only modify the damping term. The natural frequency (6) and frequency regulation capability (5) are not modified. The new damping term is given by:

$$\delta = \frac{D + k_d \omega_b K_t}{2\sqrt{2H\omega_b K_t}} \tag{10}$$

From (10) it is evident that the damping of the system can be independently adjusted to an optimal value with k_d, regardless of the values of D and H. However, although the affection of D and H can be compensated because they are known values set by the controller, the effect of the grid impedance through K_t remains still a perturbation to the damping value of the system.

To be able to fix the damping value to the optimal value for the converter operation, an adaptive method based on grid impedance estimation capability is proposed in this work. As stated in [9], this can be done in less than three fundamental frequency periods (50 ms), which is fast enough for the dynamics of typical VSG controllers. Figure 6 schematizes the adaptive modified VSG approach, considering that an impedance estimator is used to adapt the k_d term.

The impedance estimation provides $\overrightarrow{Z_g} = R_g + jX_g$ at the fundamental frequency, ω_r. If $R_c \ll X_g$, then the $K_t \cong 1/(X_c + X_g)$ and the required k_d term can be obtained to ensure the desired δ target through:

$$k_d = \frac{2\delta\sqrt{2H\omega_b K_t} - D}{\omega_b K_t} \tag{11}$$

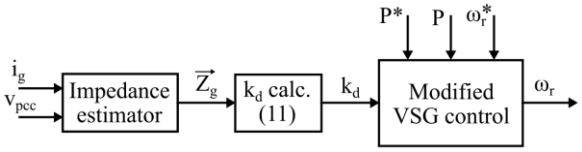

Figure 6. Modified VSG control with adaptive k_d

5. Simulation results

The modified VSG with adaptive capability is simulated in MATLAB/Simulink. The model is based on the scheme already described in Figure 1. However, the grid part has been modified in order to introduce impedance and grid frequency perturbations, as shown in Figure 7. S1 can be switched to modify the overall impedance of the grid, whereas grid frequency can be modified with a certain slew rate or rate of change of frequency. Since the target of the analysis are low frequency oscillations (< 20 Hz), averaged power electronic models are used.

Simulation parameters in per unit are gathered in Table 1, including base power, voltage and angular frequency values. The VSG is designed with an inertia constant of 5 s, and a damping term of 20. The adaptive controller is tuned to provide a k_d that ensures a minimum damping $\delta = 0.5$, regardless of the VSG parameters and grid impedance.

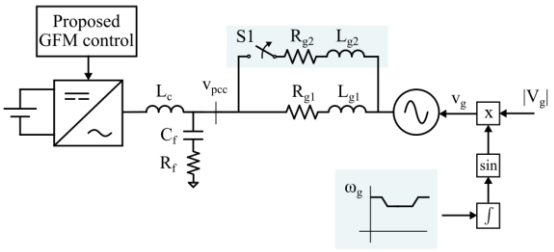

Figure 7. Simulation scheme for validating the performance of the proposed controller

Since the main goal of the work is to evaluate the performance of the controller, the impedance estimator algorithm is not implemented. Instead, the real impedance is provided to the controller. To emulate the dynamics of the estimator, a first order filter with a time constant of 250 ms is included. These dynamics are 5 times slower than state-of-the-art estimators [9]. The reactive power droop is set to $m_q = 0$. This controller will have minimum impact on the system, as the grid is mainly inductive, and only frequency perturbations are introduced.

Table 1. Simulation model parameters

Base values					
S_b	100 kW	v_b	400 V	ω_b	**50** Hz
Filter					
L_c	0.05 pu	C_f	0.05 pu	R_f	0.08 pu
R_f	0.08 pu				
Grid					
V_g	1 pu	ω_g	1 pu	X_g/R_g	5
L_{g1}	0.3 pu	L_{g2}	0.1 pu		
Controller					
H	5 s	D	20	k_d	-
τ_d	100 Hz	m_q	0		
Other parameters					
V_{dc}	1.6 pu				

The simulation starts with S1 closed. In these conditions, the grid impedance is determined by the parallel connection of the two branches, $X_{g1}//X_{g2} = 0.075$ pu and $R_{g1}//R_{g2} = 0.015$ pu. At t = 15 s, S1 is opened, and the grid impedance is increased to $X_{g1} = 0.3$ pu and $R_{g2} = 0.03$ pu. To evaluate the damping of the GFM controller under different grid conditions, two grid frequency perturbations are introduced. At t = 5 s, a frequency deviation of -0.1 Hz is applied. At t = 25 s, the grid frequency returns to the rated 50 Hz. The frequency is modified with a rate of change of frequency of 2 Hz/s. Grid frequency and reactance variation is graphed in Figure 8.

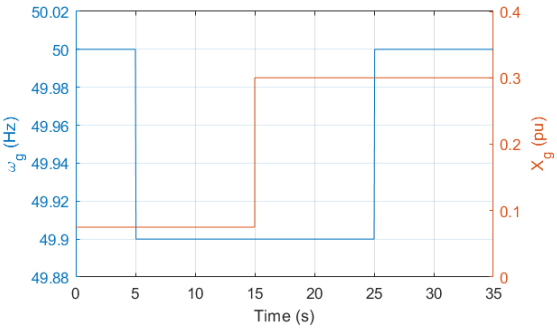

Figure 8. Grid reactance and frequency evolution during the test

The active power response of the proposed GFM controller is shown in in Figure 9. For the sake of comparison, the conventional VSG and the modified VSG without adaptive derivative term are included. In the latter, k_d is set to 0.055, which ensures a $\delta = 0.5$ at initial grid impedance conditions.

The addition of k_d provides a proper damping during the first frequency deviation. Both modified VSGs, with and without adaptive term, show the same response, as k_d has been tuned for these conditions. The original VSG, on the other hand, has a reduced damping ($\delta < 0.1$). As expected, the addition of k_d does not modify the primary frequency regulation capability of the inverter: the steady-state active power after the first grid frequency perturbation changes from 0 pu to 0.04 pu.

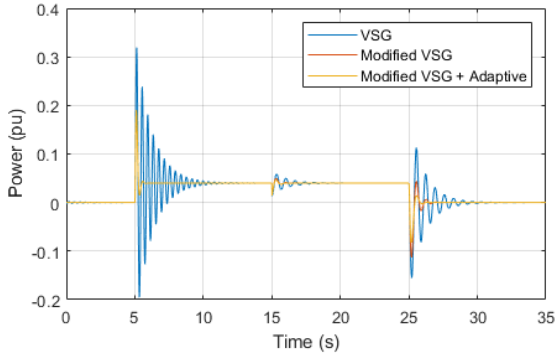

Figure 9. Active power response of the proposed VSG, compared with classical and non-adaptive VSG

Figure 10 shows a close view of the active power transient during the opening of S1. The modified VSG provides a proper damping of the transient, which reduces its settling time from around 5 s to around 1 s. The adaptive controller can improve the damping during this event, even if the dynamics of the impedance estimator have been considered much slower than state-of-the-art methods.

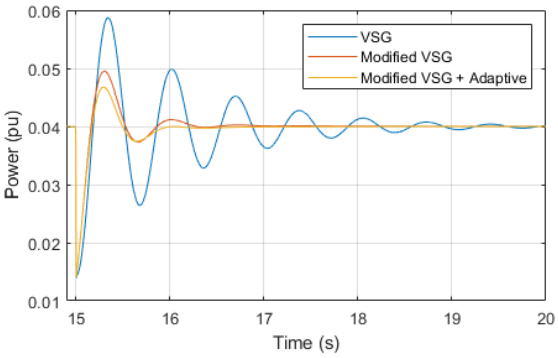

Figure 10. Close up of active power during impedance perturbation

Finally, Figure 11 shows the active power transient during the second grid frequency perturbation. This perturbation occurs with an increased grid impedance. The k_d still contributes to damp the system oscillations. However, without an adaptive controller, the damping will be deteriorated as grid impedance increases. For the simulated conditions, the damping for the fixed k_d term (Modified VSG) is reduced to 0.35. On the other hand, the

adaptive approach can ensure the required minimum damping of 0.5. Hence, adapting the derivative term shows its capability to boost the damping performance regardless of grid conditions.

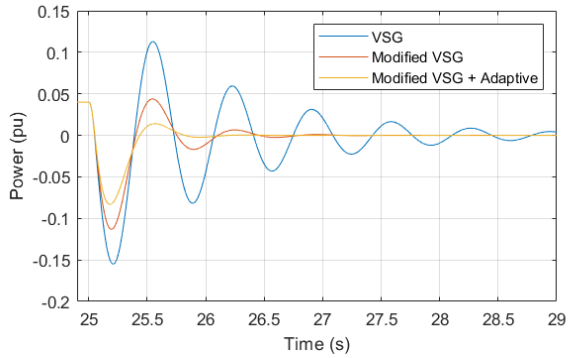

Figure 11. Close up of active power during second frequency deviation

6. Conclusions

Virtual synchronous generator is a widespread grid forming strategy which can contribute to the inertia, primary frequency regulation and damping of the grid. However, in the classical structure, these three characteristics cannot be managed independently. Hence, the damping of the inverter is usually deteriorated in high inertial or high impedance conditions. To face this issue, authors have proposed a modified VSG approach which introduces a derivative term in the active power feedback. This approach can decouple inertia, frequency regulation and the damping of the system, thanks to the additional degree of freedom. Moreover, as the damping of the system is also dependant on the grid impedance, authors have proposed a controller which can adapt its derivative term according to the estimated impedance. This strategy can ensure a minimum damping capability, regardless of the operational conditions of the GFM inverter.

Acknowledgement

This work has been supported by the Campus Bizia Lab programme (CBL 2024/2025 – 24MGOM), and the Basque Government (GISEL research group IT1522-22 and KK-2023/00042). This work has also been supported by Mobility Lab Foundation under project Territorio Verde y Sostenible (CONV23/07).

References

[1] J. Shair, H. Li, J. Hu, and X. Xie, ‘Power system stability issues, classifications and research prospects in the context of high-penetration of renewables and power electronics’, *Renewable and Sustainable Energy Reviews*, vol. 145, p. 111111, Jul. 2021, doi: 10.1016/j.rser.2021.111111.

[2] R. Aljarrah, B. B. Fawaz, Q. Salem, M. Karimi, H. Marzooghi, and R. Azizipanah-Abarghooee, ‘Issues and Challenges of Grid-Following Converters Interfacing Renewable Energy Sources in Low Inertia Systems: A Review’, *IEEE Access*, vol. 12, pp. 5534–5561, 2024, doi: 10.1109/ACCESS.2024.3349630.

[3] R. Rosso, X. Wang, M. Liserre, X. Lu, and S. Engelken, ‘Grid-Forming Converters: Control Approaches, Grid-Synchronization, and Future Trends—A Review’, *IEEE Open J. Ind. Applicat.*, vol. 2, pp. 93–109, 2021, doi: 10.1109/OJIA.2021.3074028.

[4] H. Zhang, W. Xiang, W. Lin, and J. Wen, ‘Grid Forming Converters in Renewable Energy Sources Dominated Power Grid: Control Strategy, Stability, Application, and Challenges’, *Journal of Modern Power Systems and Clean Energy*, vol. 9, no. 6, pp. 1239–1256, 2021, doi: 10.35833/MPCE.2021.000257.

[5] W. Sang, W. Guo, S. Dai, C. Tian, S. Yu, and Y. Teng, ‘Virtual Synchronous Generator, a Comprehensive Overview’, *Energies*, vol. 15, no. 17, p. 6148, Aug. 2022, doi: 10.3390/en15176148.

[6] A. Suvorov, A. Askarov, A. Kievets, and V. Rudnik, ‘A comprehensive assessment of the state-of-the-art virtual synchronous generator models’, *Electric Power Systems Research*, vol. 209, p. 108054, Aug. 2022, doi: 10.1016/j.epsr.2022.108054.

[7] H. Yin, Z. Kustanovich, J. Lin, and G. Weiss, ‘Synchronverters With Damper Windings to Attenuate Power Oscillations in Grids’, *IEEE J. Emerg. Sel. Top. Ind. Electron.*, vol. 5, no. 4, pp. 1376–1387, Oct. 2024, doi: 10.1109/JESTIE.2024.3447462.

[8] D. Liu *et al.*, ‘Improved VSG strategy of grid-forming inverters for supporting inertia and damping’, *Front. Energy Res.*, vol. 11, p. 1331024, Jan. 2024, doi: 10.3389/fenrg.2023.1331024.

[9] Oier Lopez-de-Suso *et al.*, ‘Digital Implementation Analysis of PRBS Impedance Shaping Algorithm to Estimate Multi-Sequence and Multi-Harmonic Systems’, presented at the IECON 2024 – 50th Annual Conference of the IEEE Industrial Electronics Society, 2024, pp. 1–6.

[10] I. Bennia *et al.*, ‘Design, Modeling, and Validation of Grid-Forming Inverters for Frequency Synchronization and Restoration’, *Energies*, vol. 17, no. 1, p. 59, Dec. 2023, doi: 10.3390/en17010059.

[11] A. Narula, ‘Grid-forming wind power plants’, Chalmers University of Technology, 2023. Accessed: Jun. 28, 2024. [Online]. Available: https://research.chalmers.se/en/publication/534815